

Micromachined Cavity-based Bandpass Filter and Suspended Planar Slow-wave Structure for Vacuum-microelectronic Millimeter-wave/THz Microsystem Embedded in LTCC Packaging Substrates

Min Miao^{1,2*}, Runiu Fang², Xiaoqing Zhang¹, Biao Ning¹, Fangqing Mu³, Zhensong Li¹, Wei Xiang³, and Yufeng Jin²

1. Information Microsystem Institute, Beijing Information Science and Technology University

#35, Mid North 4th Ring Road, Chaoyang District, Beijing 100101, China

Email: miaomin@bistu.edu.cn, Tel: +86-10-64884695, Fax: +86-10-64884696

2. National Key Laboratory of Science and Technology on Micro/Nano Fabrication, Peking University

#5, Yiheyuan Road, Haidian District, Beijing 100871, China

Tel: +86-10-62766591, Fax: +86-10-62755847

3. The 43rd Institute of China Electronics Technology Group Corporation.

Hefei 230088, Anhui, China

Abstract

Micromachining of ceramic packaging interposers was demonstrated by the authors in the 62nd and 63rd ECTC as one of the prospective paths leading to high-density and heterogeneous 3D integration, by showing 3 individual micromachined modules, i.e. micro-accelerometers, cooling microchannels and RF passive structures, which were fabricated on a unified platform with both LTCC SIP integration and micromachining capability. As follow ups, in this paper, initial advancements in exploring the potential of the unified platform in vacuum-microelectronic millimeter-wave/THz microsystem integration are reported, that is, the development of two 3-D micromachined millimeter-wave/THz SIP modules. Firstly, the designing, fabricating and testing of a W-band (millimeter wave) bandpass filter based on 3D micro-cavity structures is revealed, as a representative of passive millimeter wave/THz devices, which can be entirely embedded into a LTCC packaging substrate (including interposers). The test results show a mid-band (central) frequency at 88GHz and 2GHz pass-band width, a low passband attenuation of better than -3dB and a stop-band rejection of -8dB @ 5GHz off mid-band frequency (i.e. 4GHz above and below passband edges respectively) and -14dB @10GHz off mid-band frequency. Secondly, interdigitated lines screen-printed on LTCC interposer are proposed as feasible slow-wave structures that can be embedded into SIP interposers, which are the essential parts for vacuum microelectronic active devices like backward wave oscillators and travelling wave amplifiers. Full-wave electromagnetic analysis proved the effectiveness of these planar designs as slow wave micro-functional structures, showing low and smooth transmission loss and dispersion characters, as well as promising coupling impedance characters, in 5~45GHz bands. In addition, two slow-wave structures consisting of interdigitated lines suspended on LTCC membrane are proposed as improvements for higher frequency use (up to 110GHz), and full-wave analysis proves their enhanced performance and potential capability in extending the operation frequency range, maybe into the THz range. In the future, these two modules may find applications into highly integrated wireless telecommunication and radar transceivers which are now being the research and development hotspot, facilitating advanced air-borne, space-borne and high-end automotive/consumer electronics.

1. Introduction

Vacuum electronics technology has been demonstrated as an effective and sometimes indispensable way for high-end millimeter wave (MMW) through terahertz (THz) system development, especially those with features like high transmission power, large bandwidth and low dispersion [1-4]. The lack of these features in solid-state optoelectronics based solutions is now the major barrier to their wide deployment. On the other hand, although a few vacuum electronic solutions are currently available, due to the absence of effective system integration methodology, such devices and consequent systems proposed are too bulky and inefficient to be utilized in applications other than indoor security check and medical/industrial laboratory or in-line inspection. Considering the short wavelength under millimeter scale, compact 3D integrated system-in-package (SIP) with critical dimensions on millimeter scales and below, that is, a vacuum microelectronic solution, will be the optimal path to implement such systems or modules for high-end MMW through THz use, as loss, noise and other non-ideal effects due to parasitic coupling and stray may be minimized and array structures may be facilitated. Few attempts have been reported in the past few years, to fabricate modules operating in MMW through THz bands, such as backward-wave oscillators [5], by Si micromachining, LIGA or metal precision-machining. However, only a couple of these modules have shown initial performance and the machining are revealed to be unable to support cost-effective active-passive integration.

LTCC (Low Temperature Co-fired Ceramic) technology is usually considered as a significant packaging solution for traditional silicon or GaAs based RF modules for several decades, with lower cost and higher quality factor [6-8]. At the 62nd and 63rd ECTC, we have explored the potential of LTCC modules which may function as more than just packaging supports or housing, by showing 3 individual micromachined modules, i.e. micro-accelerometers, cooling microchannels and RF passive structures [9, 10]. In addition, conception of a frame-like 3D high density and heterogeneous microsystem integration scheme based on a unified LTCC package/ micromachining process platform is proposed, as the mid-to-long term target of the R&D. In this paper, the authors investigated further into the development of active and passive vacuum microelectronic structures featuring high

aspect ratio (true) 3D structures like cavity and suspended membrane, which is intended for oscillators or even transmitters for sub-MMW through THz applications.

Substrate integrated waveguide (SIW), whose process is compatible with LTCC and PCBs, was extensively explored for microwave and MMW modules, including resonator, filter, oscillator, coupler, antenna and front-end system, forming transmission or passive structures in these devices [11-13]. However, for SIW based devices operating at sub-MMW through THz frequencies, the lack of device design methodology and difficulties in their micro-fabrication are somewhat prohibitive and the performance of related LTCC modules has not been clear yet.

The rest of this paper is organized as follows. In Section II, the designing, fabricating and test results of a W-band (MMW) bandpass filter based on 3D micro-cavity structures is presented. Section III focused on micro-strip interdigitated slow-wave structures embedded in LTCC module. Finally, section IV concludes the paper.

II. The W-Band Micromachined Cavity-based Bandpass Filter

In this section, the designing, fabricating and testing of a W-band (MMW) bandpass filter based on 3D micro-cavity structures are revealed, as a representative of passive MMW/THz vacuum microelectronic devices, which can be entirely embedded into a LTCC packaging substrate. This conception has been first revealed briefly in a technical paper by the authors at the 63rd ECTC [10]. At that time, as the designing methodology had not been specialized for SIW-based devices and the fabrication process was primitive, only simulation results are available and a couple of samples are finally obtained; furthermore, the size precision is not sufficient for subsequent assembly and testing. As the design methodology and microfabrication technique matured later on, in this paper, optimized design method, process flow and SIW-based structures are adopted to provide structural design for a new application with a different operation frequency band, and a bunch of samples are prepared, sliced, assembled in a newly designed special fixture and tested.

Table 1 shows the design specifications of the W band micro-machined cavity filter. This time, the filter design consists of three parts instead of two as in [10], i.e. top cover plates, cavity section and bottom plates. Ferro A6 green tape is used in our design, and therefore the relative dielectric constant is 5.9, and the thickness of each layer is 0.096mm. For filter cavity, the most critical structure is the closed placed metal columns (SIW), each of which is formed by vertically aligning vias in the stacked-up layers of tapes. The columns surround the cavity, and thus form a quasi-continuous side-wall as a whole, from the perspective of electromagnetic field propagating. When the top and bottom cover plate is aligned with the cavity section and then soldered or glued onto it, a quasi-enclosed cavity can be formed inside the LTCC interposer, consisting of the columns and the screen-printed planar gold patterns on the top and bottom cover plates facing the cavity. Figure 1 shows the scheme of the proposed W-band cavity filter.

The equivalent circuit of the W-band filter was first generated based on ordinary filter design rules, and then transformed into design dimensions of the cavity filter. Meanwhile, the equivalent circuit models are optimized for SIW-based cavity. The dimensions were then optimized with the aid of a three dimensional full-wave electromagnetic solver, and the final dimensions of the filter are obtained as shown in Fig.2. The cavity opening, as input and output ports for the filter, is 2.54 mm in width, and 1.27mm in height (13 layers of green tapes). Fig.3 gives the finite element based full-wave simulation results of the filter, which conforms well to the designed specs of the W-band filter shown in table.1.

Table 1. The design specs of the W-band micro-machined cavity filter

specs	Mid-band frequency	Pass-band	Maximum Pass-band attenuation
	88GHz	86GHz~90GHz	$\leq 3\text{dB}$

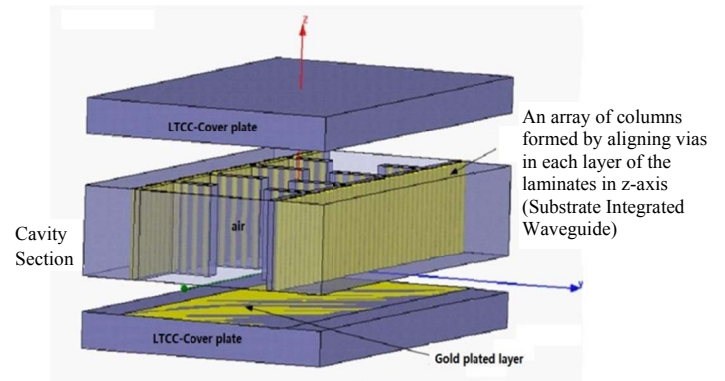


Figure 1. An explosive view of the micromachined cavity filter structure.

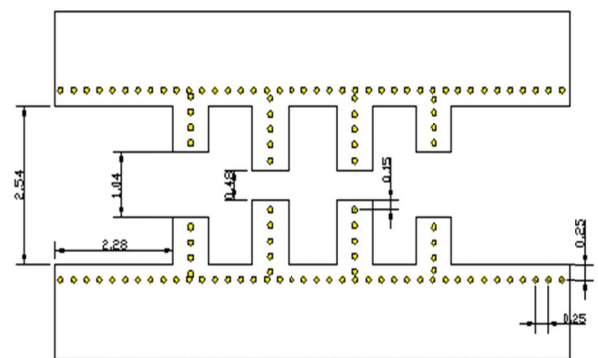


Figure 2. Dimensions of the filter cavity design (unit: mm).

The filter sample is fabricated on the unified LTCC-based micromachining and packaging platform mentioned above, and the general process flow is shown in Fig.4. The cavity section of the filter is prepared with the stacked-up 13 layers of green tapes, by micromachining perforated 2.5D patterns into the individual layers, filling them with carbon-based sacrificial materials, and laminating/sintering together to form

micro to millimeter scale 3D micro-cavity structures functioning as the basic resonant and coupling structures for the filter. During sintering, the sacrificial material is sublimated. The top and bottom cover plates are fabricated with standard LTCC laminates preparation process, with gold patterns screen-printed on the surfaces facing the cavity part. The assembling of cover plates is made in 2 steps. First, the bottom cover plate is bonded to the cavity section, and laser machining is used to cut off the diaphragm horizontally and remove their central part to form bulges and openings, and to trim the 3D microstructure as well, so that the size precision of the cavity can be further enhanced. Second, when the top cover plates are aligned with the cavity section, they are assembly together with reflow sealing or gluing, so that the filter cavity are finally formed.

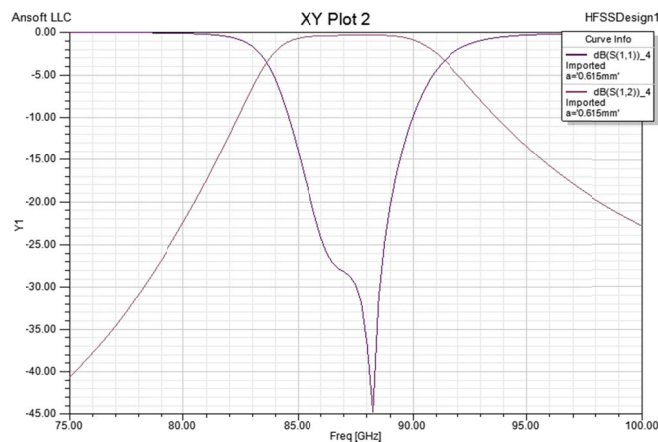


Figure 3. Finite-element method based full-wave simulation result of the W-band cavity filter design.

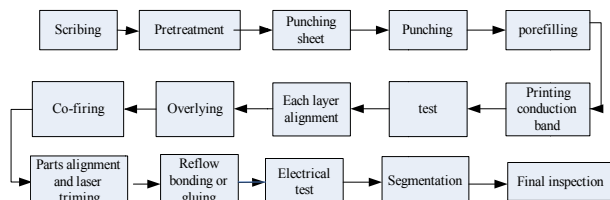


Figure 4. The manufacturing process.

The two major challenges overcome during the process development include: a) the alignment of the vias in each layer, with total misalignment under control; and b) removal of the sacrificial materials without inducing cracking or collapse of the cavity. As for the former, a refined alignment marking method is used for the lamination process, and sintering shrinkage estimation model as well as shrinkage-induced misalignment elimination algorithms is developed and adopted. In addition, an optimized sintering curve is obtained by several rounds of specially designed experiments. On the unified LTCC-based micromachining and packaging platform, the misalignment during the lamination and sintering is controlled below $\pm 5\mu\text{m}$. The consequent deviation of electrical performance was limited within acceptable levels, based on the comprehensive simulation on the effects of

process variation beforehand. Fig.5 shows the X-ray microscopy image of the W-band filter sample. The metal vias stacked up together exhibit good alignment with each other, as shown in the figure. As for the later challenge, a refined recipe of the sacrificial material is obtained by optimizing the matrix and carbon contents and sintering curve, and the samples without cracking or collapse confirm the feasibility of this enhancement.



Figure 5. X-ray microscopic image of the W-band filter. The closely placed column images, which corresponds to the vias vertically aligned together (in the 13 layers of the laminates), proves the effectiveness of the misalignment control and the integrity of the SIW formed by the stacked vias.

A special fixture is designed for the testing of the miniaturized filter, providing an appropriate and de-embeddable access to the 2 test ports of a Rohde & Schwarz Vector Network Analyzer (VNA) operating up to 110GHz. The fabricated samples and the fixture are shown in Fig. 6. A standard waveguide-flange test accessory from the VNA was selected to interface the VNA to the filter test fixture, as shown in Fig.7.

The test results, as displayed in Fig. 8, show a mid-band frequency at 88GHz and 2GHz pass bandwidth, a passband attenuation of better than -3dB and a stop-band rejection of -8dB @ 5GHz off mid-band frequency (i.e. 4GHz above and below passband edges respectively) and -14dB @10GHz off mid-band frequency. The passband width is less than expected (as compared with the simulation results shown in Fig.3). The difference between simulation and experimented results may be attributed to the existence of electromagnetic leakage and interaction between the neighboring vertical SIW columns closely placed (composing vertical cavity sidewalls), and this non-ideality may be not negligible and has not been counted for in the models adopted during the design phase.

The cavity can be utilized further as a feedthrough for patch antennas patterned on the front surface to enhance the radiation bandwidth during 3D SIP integration, which are validated with finite element full-wave analysis and will be demonstrated in another paper.

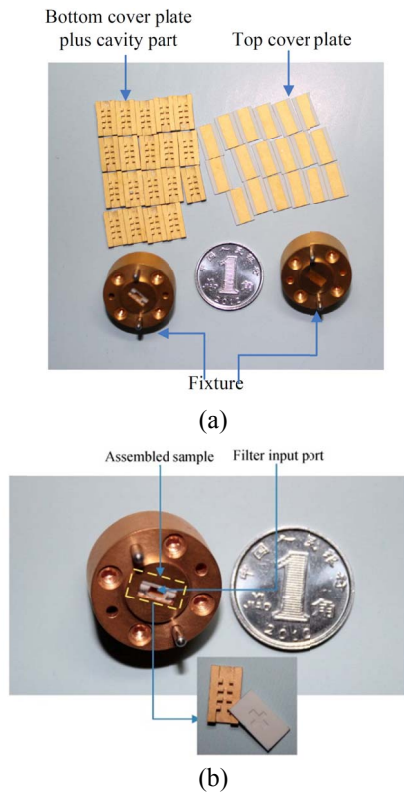


Figure 6. (a) The fabricated sample and two fixtures made of copper and plated with gold inside; (b) the fixture with a sample assembled inside.

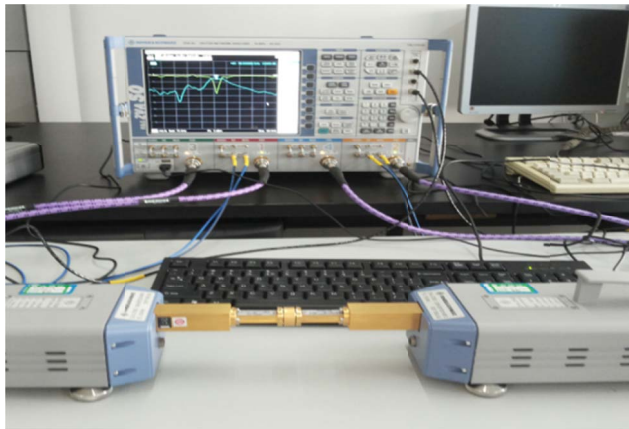


Figure 7. The test setup.

III. Micro-strip Interdigitated Slow-wave Structures Embedded in LTCC Interposers

In this section, interdigitated lines screen-printed on a solid substrate or suspended membrane embedded into LTCC interposer are proposed as slow-wave structures for vacuum microelectronics active devices like backward wave oscillators and travelling wave amplifiers. Slow wave structures based on interdigitated lines have several advantages, including simple structure design and manufacturing process, and low operating voltage for strong interaction between electron beam and slowed travelling electromagnetic wave [14]. A new micro-strip interdigitated

line design for slow-wave structure based on LTCC process is schematically presented, as shown in Fig. 9.

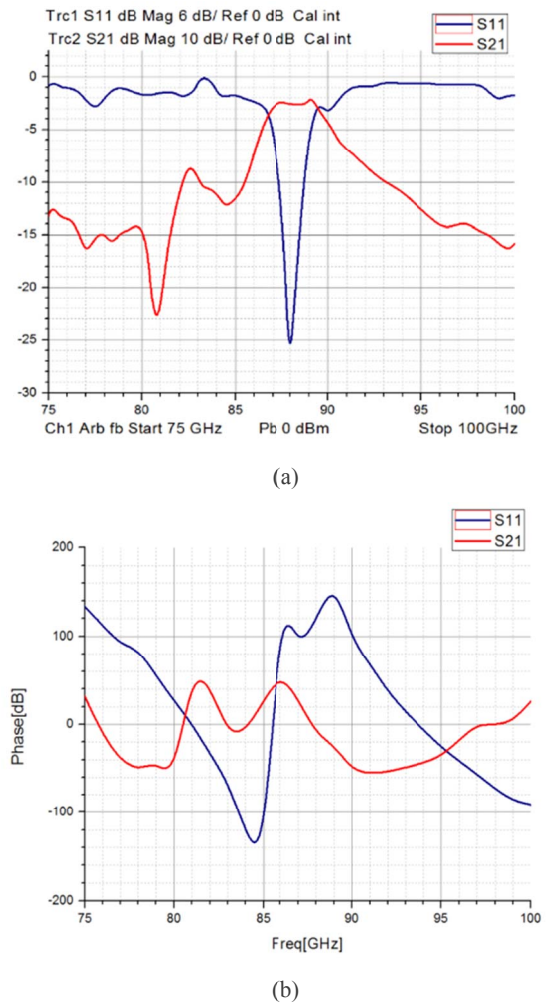


Figure 8. The test results of the filter (a) the amplitude-frequency characteristic (b) the phase-frequency characteristic diagram.

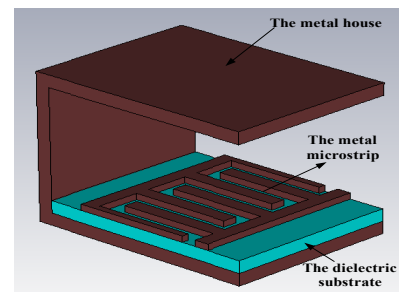


Figure 9. Micro-strip interdigitated lines as the slow-wave structure (substrate interdigitated lines, SIDL).

A three-dimensional full-wave electromagnetic solver based on finite integration method was applied to extract the

cold test characteristics. First of all, the effects of structural parameters on the cold test characteristics are analyzed, including thickness, space and length of interdigitated lines. As shown in Fig.10, the dispersion is mainly affected by width and length of interdigitated lines, and the coupling impedance is mainly affected by thickness and length of interdigitated lines.

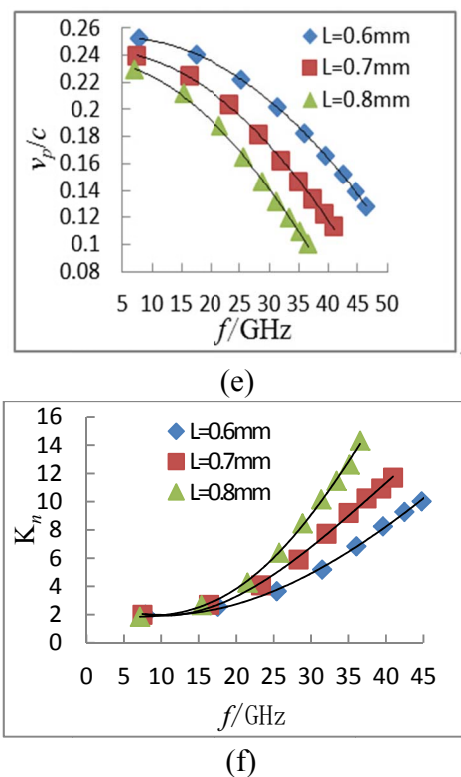
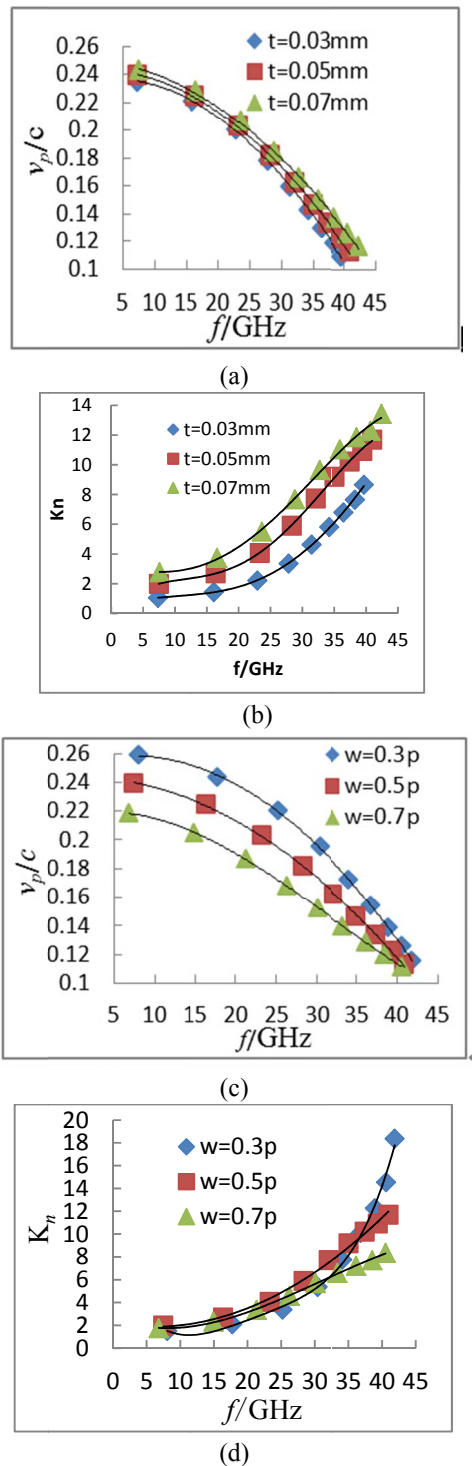
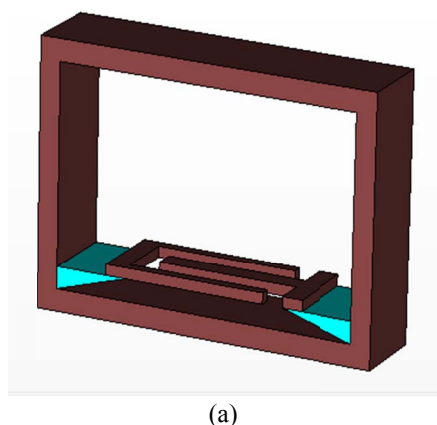


Figure 10. Effect of variation of structural parameters on dispersion and coupling impedance: (a) thickness of interdigitated lines on dispersion; (b) thickness of interdigitated lines on coupling impedance; (c) width of interdigitated lines on dispersion; (d) width of interdigitated lines on coupling impedance; (e) length of interdigitated lines on dispersion; (f) length of interdigitated lines on coupling impedance.

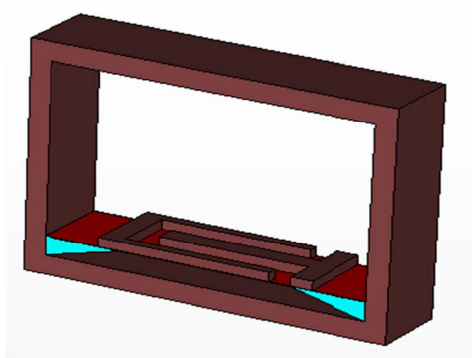
In order to minimize dielectric loss incurred by LTCC material, two improved slow-wave structures are proposed and analyzed, i.e. the free interdigital line (FIDL) and the membrane inter-digital line (MIDL), as shown in the Fig.11. For both structures, the substrate dielectric below the interdigitated lines is excavated, and under MIDL an additional $2\mu\text{m}$ thick membrane is deposited to enhance the mechanical support under the slow-wave structure. Comparative simulations on cold test characteristics are carried out between the two improved slow-wave structure designs and the interdigitated lines directly on interposers, i.e. SIDL. As shown in the Fig.12, the dispersion and coupling impedance of MIDL and FIDL are significantly improved compared with SIDL. Therefore, the operating frequency range can be extended with MIDL and FIDL. Besides, the coupling impedance is higher for MIDL and FIDL, which signifies a high energy transitional rate between electron beam and electromagnetic wave.

The process development for the suspended interdigitated metal strips is not quite a challenge. The metal house can be made with metal frame soldering onto the surface of interposers in combination with the parallel-seam welding of the top cover metal plate onto the top of frame [9]. The suspended membrane can be implemented with a process introduced in reference [10], which has fabricated a patterned

suspended membrane structure that can be embedded into an interposer, i.e. the proof mass and suspension spring of a micro-accelerometer.



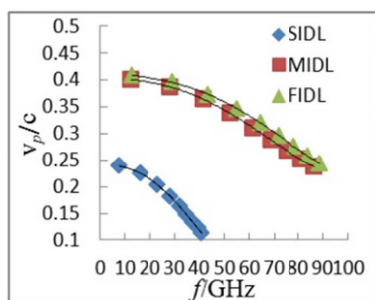
(a)



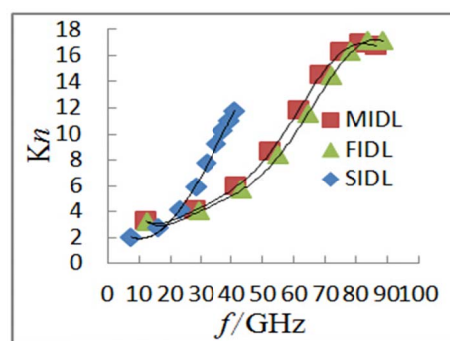
(b)

Figure 11. Improved slow-wave structures which are suspended: (a) free interdigital lines (FIDL) (b) membrane inter-digital lines(MIDL)

In all, the planar slow wave design shown above enables potentials of compact 3D integration of vacuum-microelectronic active and passive structures operating at MMW frequencies and above. In addition, active control and RF driving IC can be surface mounted onto the interposer and connected to the embedded vacuum-microelectronic devices, in a cost effective way.



(a)



(b)

Figure 12. Cold test characteristics of substrate interdigitated lines (SIDL), free interdigitated lines (FIDL), and membrane interdigitated lines (MIDL): (a)dispersion (b)coupling impedance.

IV. Conclusions

In this paper, the advancements of compact 3-D millimeter-wave/THz SIP modules are presented based on the unified platform with both SIP integration and micromachining capability. First of all, the designing, fabricating and testing of a W-band bandpass filter based on 3D micro-cavity structures are revealed, as a representative of passive MMW/THz devices, which can be entirely embedded into a LTCC packaging substrate (including interposer). The test results show a mid-band (central) frequency at 88GHz and 2GHz pass-band width, a passband attenuation of better than -3dB and a stop-band rejection of -8dB @ 5GHz off mid-band frequency (i.e. 4GHz above and below passband edges respectively) and -14dB @10GHz off mid-band frequency. Secondly, interdigitated lines screen-printed on LTCC interposer are proposed as feasible slow-wave structures, which are the essential part for vacuum microelectronics active devices like backward wave oscillators and travelling wave amplifiers. Full-wave electromagnetic analysis proves the effectiveness of these planar designs as slow wave micro-functional structures, showing low and smooth transmission loss and dispersion characters, as well as promising coupling impedance characters, in 5~45GHz bands. In addition, two suspended slow-wave structures are proposed for the improvement of interdigitated lines for higher frequency (up to 110GHz) use, and EM full-wave analysis prove their enhanced performance and potential capability in extending the operation frequency. In the future, these modules may find applications into highly integrated wireless telecommunication and radar transceivers which are now being the research and development hotspot, facilitating advanced air-borne, space-borne and high-end automotive/consumer electronics.

Acknowledgments

The work presented here has been funded by National Natural Science Foundation of China (Project No. 61176102, 60976083 and 60501007), The Importation and Development of High-Caliber Talents Project of Beijing Municipal Institutions (Great Wall Scholar, No. CIT&TCD20150320), and Beijing Natural Science Foundation (Project No.

3102014), China. In addition, research funding from National S&T Major Project with the contract No. 2009ZX02038 is greatly acknowledged.

References

1. Yeo, K.S., *et al*, "Contious Wave Tunable Fiber Optical Parametric Oscillator with Double-pass Pump Configuration," *Applied Physics B*, Vol. 110, No.3 (2013), pp. 353-357.
2. He, W. , *et al*, "High Power Wideband Gyrotron Backward Wave Oscillator Operating towards the Terahertz region," *Physical Review Letters*, Vol.110, No.16 (2013), pp.165101.
3. Liu, L.W., *et al*, "Research on Novel Slotted Helix Slow-Wave Structure for High Power Ka-Band Traveling-Wave Tube," *Chinese Physics B*, Vol.08, No.3 (2013), pp.102-113.
4. Lai, J. Q., *et al*, "Design and Simulation of 140 GHz High Power Staggered Double Vane Traveling-Wave Tube". *Journal of Physics*, Vol. 61, No.17 (2012), pp.545-552.
5. Feng, J. J., *et al*, "The 340GHz THz Backward Wave Oscillator," *Jornal of Terahertz Science and Electronic Information Technology*, Vol. 11, No.1 (2013), pp. 32-37.
6. Peters, F., *et al*, "Two layer LTCC Substrate Integrated to Rectangular Waveguide Transition and its Application for Millimeter-wave LTCC Characterization," *Micro. Opt. Technol. Lett.*, Vol. 54, No. 2 (2012), pp.1896-1908.
7. Zhou J., "Towards Rational Design of Low-Temperature Co-Fired Ceramic (LTCC) Materials," *Journal of Advanced Ceramics*, Vol. 1, No.2 (2012), pp.89-99.
8. Miao M., *et al*, "Design and Simulation of THz Filters Embedded in LTCC Multi-layer Substrate," *2011 Intl. Conf. on Electron Devices and Solid-state Circuits(EDSSSC)*, Tianjin, China, Nov. 2011, pp.1-4.
9. Miao, M., *et al*, "Investigation of a Unified LTCC-based Micromachining and Packaging Platform for High Density/multifunctional Microsystem Integration," *IEEE 62nd. Electronic Components and Technology Conference (ECTC)*, San Diego, CA, May. 2012, pp. 377-384.
10. Miao, M., *et al*, "Investigation of Micromachined LTCC Functional Modules for High-density 3D SIP Based on LTCC Packaging Platform," *IEEE 63rd Electronic Components and Technology Conference (ECTC)*, Las Vegas, NV, May. 2013, pp.1815-1822.
11. Shen, T. M., *et al*, "Design of Vertically Stacked Waveguide Filters in LTCC," *IEEE Trans. Microwave Theory. Tech*, Vol. 55, No.8 (2007), pp.1771-1779.
12. Ren, H., *et al*, "The Design and Simulation of the LTCC Multilayer Microwave Bandpass Filter," *The Fourteenth Electronic Components Symposium of the Chinese Electronic Society*, 2006, pp.210-213.
13. Zhou, S. R., *et al*, "The Research of the Plate Multilayer Three Terminal Ceramic EMI Filter," *Electronic Components and Materials*, Vol. 21, No. 2 (2002), pp. 22-24.
14. Kory C., *et al*, "Novel TWT Interaction Circuits for High Frequency Application", *IVEC2004*, pp.51-52.